

# Superconductivity in the Extended Hubbard Model with More Than Nearest-Neighbour Contributions

Zsolt Szabó and Zsolt Gulácsi

*Department of Theoretical Physics, Lajos Kossuth University,  
H-4010 Debrecen, P.O. Box 5., Hungary*

(June 23, 2021)

Superconducting phase diagram of the extended Hubbard model supplemented with interaction and hopping terms exceeding nearest neighbour distance in range is analysed systematically at different band-filling and temperature values in a mean-field approximation. The obtained results clearly underline the importance of next-nearest neighbour terms in developing the main superconducting properties of the model system. In particular, the emergence of superconducting phases of different symmetry at a given point of the phase diagram, critical temperatures  $T_c$ , zero temperature gap amplitude values  $\Delta_0$ ,  $\Delta_0/T_c$  ratios, doping and temperature dependences are all strongly influenced by next-nearest neighbour contributions.

## I. INTRODUCTION

The subject of high critical temperature superconductors starting from an early proposal of Anderson (Anderson, 1987) polarizes significant forces around the Hubbard model, its extensions and derivatives (Dagotto, 1994). On this line, taking the fact into account that high temperature superconductivity generally emerges in systems with a pronounced planar structure (Smith, Manthiram, Zhou, Goodenough and Market, 1991), the two-dimensional square lattice version of the Hubbard model in its extended version is intensively used as a starting point for describing superconducting properties of this type of materials (Micnas, Ranninger and Robaszkiewicz, 1990). As a consequence, within the last few years the Hubbard Hamiltonian containing nearest neighbour ( $NN$ ) interaction and hopping terms, has been extensively studied (de Boer, de Chatel, Franse and de Visser, 1995) and the emergence of superconductivity has been rigorously demonstrated in some conditions (de Boer, Korepin and Schadschneider, 1995) in these systems. In the last period, however, a great number of results directed our attention to the importance of extending the interaction and hopping range in such type of an analysis. The stimulating observations can be summarized as follows.

Concerning the kinetic energy term, Koma and Tasaki starting from the approximation-free study of two-point correlation functions at finite temperatures in low dimensional extended Hubbard models containing more than  $NN$  hopping terms (Koma and Tasaki, 1992) sharply demonstrated the fact that electron hopping with higher than  $NN$  terms plays a fundamental role in various condensation phenomena in itinerant-electron systems. The importance of hopping-range in building up the phase diagram was also emphasized in an exact manner for finite- (Tasaki, 1995) and infinite- $U$  (Verges, Guinea, Galan, van Dongen, Chiappe and Louis, 1994) Hubbard models. Furthermore, as it was pointed out by Veilleux *et al.* (Veilleux, Daré, Chen, Vilk and Tremblay, 1995) within a model containing only  $NN$  hopping the Fermi surface topology and the filling dependence of both the Hall coefficient and the uniform magnetic susceptibility are qualitatively wrong, a disagreement that cannot be removed perturbatively. On the other hand, incorporating also next-nearest neighbour ( $NNN$ ) hopping the band structure becomes more realistic and all the above mentioned physical quantities, as well as the position of neutron scattering intensity maxima, have the correct qualitative behaviour (Lavagna and Stemann, 1994, Littlewood, Zaanen, Aeppli and Monien, 1994). Following this line of reasoning it is important to mention that the relative influence of density of state (DOS) effects - like van Hove singularities (Blumberg, Stojkovic and Klein, 1995) - and Fermi surface topology effects - like nesting (Gulácsi, Bishop and Gulácsi, 1995) - on pairing are extremely important in describing superconducting properties of high- $T_c$  materials. While both van Hove singularity and nesting occur simultaneously at half filling in the usual  $NN$  model, there is no nesting when  $NNN$  hopping is present (Veilleux *et al.* and references cited therein) and the influence of saddle point effects (Abrikosov, 1995, Abrikosov, 1994) can be taken more accurately into consideration. Furthermore, the presence of hopping exceeding  $NN$  terms in range was observed, in particular, by thermopower measurements in related systems (Ponnambalam and Varadaraju, 1995) and was found to be consistent with angle-resolved photoemission data (Fehrenbacher and Norman, 1995) and gap symmetry analysis (O'Donovan and Carbotte, 1995) too. We also would like to mention that the ratio of  $NN$  to  $NNN$  hopping amplitudes is clearly known for a broad spectrum of high- $T_c$  materials (Brenig, 1995).

Concerning the interaction terms, it is known from exact studies of phase diagrams related to extended Hubbard models in higher than one dimension (Strack and Vollhardt, 1994) that contributions exceeding  $NN$  distances in range can significantly influence the emergence of condensed phases. Up to this moment such type of studies have

been carried out on magnetic phases, however, the relevance of the obtained results to superconductivity is quite straightforward (Strack and Vollhardt, 1995). Similarly, the non-negligible character of  $NNN$  interaction contributions was clearly pointed out experimentally. For example, the importance of  $NNN$  type off-site interactions was revealed in the interpretation of Auger core-valence line shapes (Verdozzi and Cini, 1995), which allows the direct observation and measurement of interparticle interaction strength and its distance dependence in valence bands of solids (Verdozzi, 1993). Furthermore, King *et al.* based on angle resolved photoemission data (King *et al.*, 1993), clearly underline that model Hamiltonians containing interaction terms only up to the  $NN$  ones are not sufficient for the proper description of the electronic structure near the Fermi energy ( $E_F$ ) in  $NCCO$  type materials. They also conclude that  $NNN$  interactions are *very* important and models including only  $NN$  interactions in  $CuO_2$  planes are unable to explain related clear experimental facts. The interpretation of two-magnon Raman scattering in high- $T_c$  materials (specially the  $A_{1g}$  and  $B_{2g}$  finite intensity peaks) also requires second-nearest neighbour or even longer-range contributions to be incorporated at the level of the interaction terms (Brenig). Moreover, the importance of  $NNN$  terms in developing basic properties of extended Hubbard models has been claimed (Di Stasio and Zotos, 1995), their effect on screening processes and as well as on phase diagram configurations has been studied (van den Brink, Meinders, Lorenzana, Eder and Sawatzky, 1995), the relevance to  $YBCO$  materials has been emphasized for various conditions (Grigelionis, Tornau and Rosengren, 1996) and their importance in loss of antiferromagnetic order has been discussed (Kampf, 1994).

Stimulated by these findings we present an extensive study of superconducting phase diagram of the extended Hubbard model containing more than nearest neighbour contributions, in order to provide a systematic image about the importance of the longer range contributions. The study is given in two dimensions, based on a traditional Hartree-Fock type decoupling procedure in terms of the Green's function description allowing, however, arbitrary gap symmetry. The DOS is treated exactly, and the stable superconducting state is chosen on the basis of a free-energy type analysis. Such type of a *systematic* investigation, incorporating the effects of  $NNN$  terms too, has not been presented so far in literature.

Our results emphasize the importance of interaction and hopping terms *exceeding* nearest neighbouring distance in range in building up superconducting characteristics of the system described by an extended Hubbard type model. In particular, the emergence of superconducting phases of different symmetry at a given point of the phase diagram, critical temperatures, zero temperature gap amplitude values,  $\Delta_0/T_c$  ratios, doping and temperature dependences are strongly influenced by the presence of  $NNN$  terms. Based on the results we conclude that the effect of  $NNN$  terms is not marginal but essential in the description of basic superconducting properties.

The paper is organized as follows. Section II presents the model, Sec. III contains besides the numerical procedure (Sec. III A) the obtained results grouped into three paragraphs as follows: Sec. III B analyzes the  $NN$  case, Sec. III C outlines the effect of hopping terms exceeding  $NN$  distances in range and Sec. III D presents the effects of  $NNN$  interaction contributions, the study being given at various temperature and doping values. Finally, the conclusions and summary close the presentation in Sec. IV.

## II. THE MODEL AND ITS DESCRIPTION

In this paper the following extended Hubbard Hamiltonian is considered on a square lattice:

$$H = - \sum_{i,j} \sum_{\sigma} t_{ij} c_{i\sigma}^{\dagger} c_{j\sigma} + \frac{1}{2} \sum_{i,j} \sum_{\sigma,\sigma'} U_{ij}^{\sigma\sigma'} n_{i\sigma} n_{j\sigma'} , \quad (1)$$

where the fermion operators  $c_{i\sigma}^{\dagger}$  and  $c_{i\sigma}$  create and annihilate, respectively, electrons with spin  $\sigma$  in the single tight-binding orbital associated with site  $i$ , and  $n_{i\sigma}$  is the particle number operator. The parameters  $t_l \equiv t_{ij}$  with  $l = 1, 2, \dots, 5$  are the real space hopping matrix elements between sites  $i$  and  $j$  with a diagonal part  $t_0 \equiv t_{ii}$ . The coupling constants  $U_{ij}^{\sigma\sigma'}$  are independent parameters denoted below as  $U_0 \equiv U_{ii}^{\sigma\sigma'}$ ,  $U_1 \equiv U_{i,i+1}^{\sigma\sigma'}$  and  $U_2 \equiv U_{i,i+2}^{\sigma\sigma'}$  on-site, nearest neighbour and next-nearest neighbour contributions, respectively. All higher order interaction terms (for  $j > i+2$ ) will be neglected for the present study, that is,  $U_l \equiv U_{i,j>i+2}^{\sigma\sigma'} = 0$ . Furthermore, any of  $U_0$ ,  $U_1$  and  $U_2$  can either be positive or negative with no further restriction. This general choice of interaction constants allows us a systematic exploration of the full superconducting phase diagram of the model under study.

The gap equation obtained within a Hartree-Fock decoupling procedure (Abrikosov, Gor'kov and Dzyaloshinskii, 1965) is given by

$$\Delta(\vec{k}) = - \sum_{\vec{q}} U(\vec{q} - \vec{k}) \Delta(\vec{q}) F(\vec{q}) , \quad (2)$$

and the chemical potential  $\mu$  is controlled via

$$1 - \delta = \sum_{\vec{k}} \left( 1 + \Omega(\vec{k}) F(\vec{k}) \right) . \quad (3)$$

Here  $\delta = 1 - 2n$  is the band filling factor with positive or negative values corresponding to hole or electron doping, respectively. Furthermore,  $n$  is the particle number density for a given spin index. In the above equations

$$F(\vec{k}) = \frac{\tanh(\frac{1}{2} \beta E(\vec{k}))}{2 E(\vec{k})} , \quad (4)$$

$$E(\vec{k}) = \sqrt{\Omega^2(\vec{k}) + \Delta^2(\vec{k})} , \quad (5)$$

$$\Omega(\vec{k}) = \mu - \epsilon(\vec{k}) - n \bar{U} , \quad (6)$$

with  $\bar{U} = U_0 + 8U_1 + 8U_2$ , and  $\beta$  stands for the reciprocal temperature. Taking the lattice spacing to be unity, the explicit expression of the inter-particle coupling in  $\mathbf{k}$ -space for a square lattice is given by

$$U(\vec{k}) = U_0 + 2U_1 (\cos k_x + \cos k_y) + 4U_2 \cos k_x \cos k_y . \quad (7)$$

One can easily verify that in Eq. (2)

$$U(\vec{q} - \vec{k}) = \sum_{i \in \mathcal{R}} g_i \Psi_i(\vec{k}) \Psi_i(\vec{q}) , \quad (8)$$

where  $\mathcal{R}$  collects all the irreducible representations of the point group ( $C_{4v}$ ) characterizing the square lattice,  $\Psi_i(\vec{k})$  represents the basis functions of the  $i$ th irreducible representation and  $g_i$  denotes the effective coupling constants (see Table I). As a consequence, the  $\mathbf{k}$ -dependent order parameter can be given in terms of these basis functions, that is,

$$\Delta(\vec{k}) = \sum_{i \in \mathcal{R}} \Delta_i \Psi_i(\vec{k}) . \quad (9)$$

In Eq. (9)  $i$  represents both singlet and triplet pairing. Based on Eqs. (2) and (9) the gap amplitudes can be written as

$$\Delta_i = -g_i \sum_{j \in \mathcal{R}} \Delta_j \sum_{\vec{k}} F(\vec{k}) \Psi_i(\vec{k}) \Psi_j(\vec{k}) \quad (10)$$

for each irreducible representation  $i$ . In case of representations  $B_1$  and  $B_2$  the gap equation is scalar, while for representation  $A_1$  we have to solve a coupled system consisting of three equations due to mixing of the corresponding three basis functions. A similar situation emerges for triplet pairing where two equations are coupled together since the corresponding irreducible representation of the states are two-dimensional.

TABLE I. The basis functions  $\Psi_i(\vec{k})$  and their notations, representations and the corresponding effective coupling constant  $g_i$  entering the pair potential.

$\mathcal{R}$	$\Psi_i(\vec{k})$	notation	$g_i$
$A_1$	1	$s$	$U_0$
$A_1$	$\frac{1}{2}(\cos k_x + \cos k_y)$	$s^*$	$4U_1$
$A_1$	$\cos k_x \cos k_y$	$s_{xy}$	$4U_2$
$B_1$	$\frac{1}{2}(\cos k_x - \cos k_y)$	$d_{x^2-y^2}$	$4U_1$
$B_2$	$\sin k_x \sin k_y$	$d_{xy}$	$4U_2$
$E$	$\frac{1}{2} \begin{pmatrix} \sin k_x + \sin k_y \\ \sin k_x - \sin k_y \end{pmatrix}$	$\begin{pmatrix} p \\ \tilde{p} \end{pmatrix}$	$4U_1$
$E$	$\frac{1}{2} \begin{pmatrix} \sin k_x \cos k_y + \sin k_y \cos k_x \\ \sin k_x \cos k_y - \sin k_y \cos k_x \end{pmatrix}$	$\begin{pmatrix} p_2 \\ \tilde{p}_2 \end{pmatrix}$	$8U_2$

The dispersion relation is given in terms of the real space hopping matrix elements as

$$\epsilon(\vec{k}) = t_0 + \sum_l t_l \exp(i\vec{k}\vec{R}_{i,i+l}), \quad (11)$$

where  $\vec{R}_{i,i+l}$  denotes lattice vector pointing from site  $i$  to its  $l^{th}$  neighbour ( $l \geq 1$ ).

At a given temperature all the possible ordered phases can be found as the nontrivial solutions of Eqs. (2) and (3). After the self-consistent solution, the stability of ordered phases of different symmetry was carefully investigated. This has been performed on the basis of a comparative free-energy (or at  $T = 0$  internal energy) analysis (for the procedure see eg. (Dahm, Erdmenger, Scharnberg and Rieck, 1993)). If the gap-equation presented more possible solutions connected to the same point of the phase diagram, the free-energy of each solution was determined and compared. For any solution, the free-energy relative to the normal state per particle  $\delta F$ , can be derived by improving the method of Gyorffy *et al.* (Gyorffy, Staunton and Stocks, 1991), the final result being given by

$$\begin{aligned} \delta F[\Delta(\vec{k}), \mu, T] = & - \sum_{\vec{k}} \left\{ E(\vec{k}) - |\Omega(\vec{k})| \right\} + 2 \sum_{\vec{k}} \left\{ \Delta^2(\vec{k}) F(\vec{k}) - \frac{1}{\beta} \ln \frac{1 + e^{-\beta E(\vec{k})}}{1 + e^{-\beta |\Omega(\vec{k})|}} \right\} \\ & + \sum_{\vec{k}} \sum_{\vec{q}} \Delta(\vec{q}) F(\vec{q}) U(\vec{q} - \vec{k}) \Delta(\vec{k}) F(\vec{k}). \end{aligned} \quad (12)$$

In this manner, altering the interaction parameters, the superconducting phase diagram of the present model has been constructed systematically at different temperature and band-filling values and main superconducting characteristics have been studied in every phase diagram domain in detail.

### III. THE OBTAINED RESULTS

#### A. Numerical procedure

To construct a phase diagram as presented above, first Eqs. (3) and (10) have been solved for the amplitudes  $\Delta_i$  corresponding to different representations. Since the factor  $F(\vec{k})$  occurring in these equations depends on all the  $\Delta_i$  values, a self-consistent procedure has to be applied. This requirement has been fulfilled by the adoption of Broyden's algorithm (Numerical Recipes in Fortran, 1992), which assures the global convergence.

To start the algorithm, first a vector composed of  $\Delta_i$  and  $\mu$  denoted by  $\underline{\Delta}_i^{(1)}$  is picked up arbitrarily at the fixed  $T$ ,  $n$  and  $g_i$  values. At this choice the possibility of mixing different symmetry representations is allowed with no restrictions. Then using this point as a zeroth guess for the solution of Eqs. (3) and (10) the nonlinear set of equations is solved numerically in order to get  $\underline{\Delta}_f^{(1)}$ . In the knowledge of  $\underline{\Delta}_f^{(1)}$  the initial guess for the next iteration  $\underline{\Delta}_i^{(2)}$  can be constructed in terms of the linear combination of  $\underline{\Delta}_i^{(1)}$  and  $\underline{\Delta}_f^{(1)}$ . This linear combination provides the global nature of convergence (i.e. directional dependences are eliminated and the solution does not depend on the starting  $\underline{\Delta}_i^{(1)}$  value). Then, using  $\underline{\Delta}_i^{(2)}$  as a starting point for the next iteration ( $m = 2$ ), the equations are solved again to obtain  $\underline{\Delta}_f^{(2)}$ , in terms of which the starting point for the 3rd iteration  $\underline{\Delta}_i^{(3)}$  can be constructed, and so on. The above procedure is continued until self-consistency has been reached, that is, until at the end of the  $m$ th iteration the difference  $\epsilon_m = |\underline{\Delta}_f^{(m)} - \underline{\Delta}_i^{(m)}|$  is less than a small, positive and *a priori* fixed value,  $\epsilon$ . In the present calculation  $\epsilon$  is chosen to be  $10^{-6}$ . The required convergence is fulfilled in average after  $m \sim 25 - 30$  iterations for the chosen value of  $\epsilon$ .

Because of the complexity of this analysis, only the possible superconducting phases were considered (i.e. the possible emergence of spin (*SDW*) and charge (*CDW*) density wave type phases was discussed, although it was not investigated systematically in detail).

#### B. Hamiltonian with nearest neighbour terms only

We started our study with the analysis of pure *NN*-case where  $U_2 = 0$  is satisfied and non-vanishing hopping matrix elements were taken into consideration only between nearest neighbouring sites, that is,  $t_l \neq 0$  for  $l = 1$  and  $t_l = 0$

otherwise. In what follows, all the couplings are normalized by the bandwidth,  $W = 8t_1$  (for example, in the case of *Bi2212* we have  $W = 1.192$  eV extracted from *ARPES* data). The obtained results are plotted in Fig. 1. Here four separate plots are presented at zero (Fig. 1(a) and (c)) and nonzero (Fig. 1(b) and (d)) temperatures for half filling ( $\delta = 0.0$ , Fig. 1(a),(b)) and away from half filling ( $\delta \neq 0.0$ , Fig. 1(c),(d)).

Concerning the notations, *paramagnetic* refers to the normal state of the model, *d-wave* and *p-wave* stand for order parameters with  $(\cos k_x - \cos k_y)$  and  $(\sin k_x + \sin k_y)$   $\mathbf{k}$ -dependence, respectively, while  $A_1$  denoting the  $A_1$ -symmetry solution of the gap equations represents in this paragraph (in Fig. 1) a standard *s*-wave component for plots (a) and (b), and an  $(s, s^*)$  admixture for plots (c) and (d). Here  $s^*$  stands for the extended *s*-wave solution.

In Fig. 1(a) the  $T = 0$  ground state phase diagram at half-filling is shown. As it can be seen, if either the on-site  $U_0$  or the intersite  $U_1$  interaction is attractive superconductivity emerges, where the symmetry of the stable, ordered phase revealed by the  $\delta F$  analysis is  $A_1$ - or  $d_{x^2-y^2}$  for reasonable values of  $|U_1/W|$ . Furthermore, if both interaction parameters are attractive a competition between different symmetry pairing states is observed. It can also be seen that increasing the value of  $|U_0|$ , triplet pairing is no longer favored. This means particularly, that repulsive on-site interaction stabilizes the superconducting state of  $d_{x^2-y^2}$ -symmetry.

Comparing these facts with the preliminary results of Micnas *et al.*, a qualitative agreement can be observed. Here we should mention that taking spin and charge density wave ordering possibilities also into account, the paramagnetic region of Fig. 1(a) can be filled up by these phases not affecting the main superconducting regions of the plot. However, the occurrence of pure  $d_{x^2-y^2}$  state instead of an *s*-*d* mixture (Micnas, Ranninger, Robaszkiewicz and Tabor, 1988, Micnas, J. Ranninger and S. Robaszkiewicz, 1989) is found in Fig. 1.a, which is in accordance with the results of Fehrenbacher and Norman (Fehrenbacher *et al.*), O'Donovan and Carbotte (O'Donovan *et al.*) and also with group-theoretical studies (Wenger and Östlund, 1993).

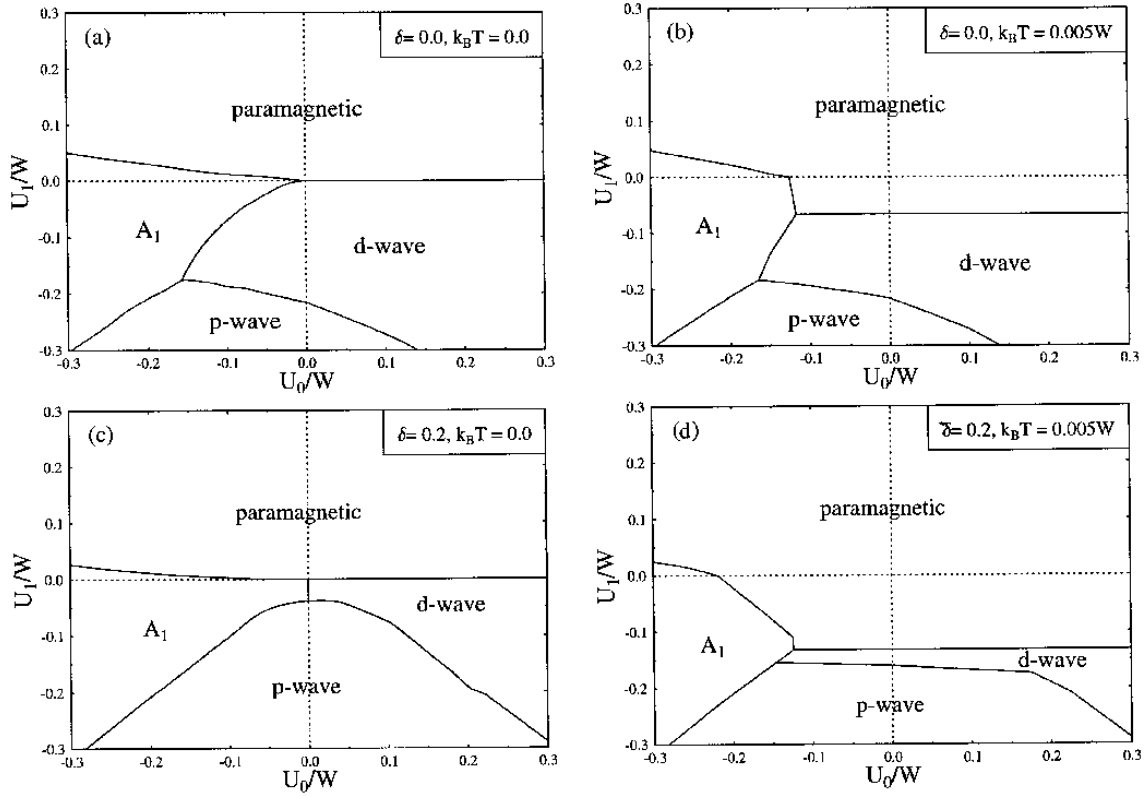


FIG. 1. Nearest-neighbour phase diagram at zero ( $k_B T = 0.0$ ) and nonzero ( $k_B T = 0.005W$ ) temperatures for different dopings ( $\delta$ ), using dispersion containing only nearest neighbour hopping terms. Dotted lines mean coordinate axis, solid lines represent boundaries between different symmetry phases. For notations  $A_1$ , *d*, *p*, and *paramagnetic* see the text.

With the non half-filled band case at zero temperature (Fig. 1(c) at  $\delta = 0.2$ ), we start to explore a parameter domain of the phase diagram which has not been investigated *systematically* so far in the literature. As it can be seen from the plot, the symmetry of the pairing state is strongly doping dependent; the  $A_1$ - and *p*-wave solutions, with increasing  $\delta$ , are gradually overwhelming the superconducting phase of  $d_{x^2-y^2}$  symmetry, as it is predicted by Micnas *et al.*. On the other hand, moving away from half-filling an  $s^*$  component of the  $A_1$ -symmetry solution sets in, suggesting that

the rigorous constraints on  $s$ -wave pairing deduced by Zhang for the standard Hubbard model with on-site interaction only (Zhang, 1990), is also applicable in the extended Hubbard model case.

The  $T \neq 0$  counterparts of Fig. 1(a) and (c) are Fig. 1(b) and (d), respectively, keeping the same notations for the labeling of superconducting phases. In Fig. 1(b) the phase diagram for the half-filled band is depicted. It can be observed, around  $|U_0/W| \approx 0.15$ , that with increasing temperature the stable  $A_1$ - and  $d_{x^2-y^2}$ -symmetry superconducting phases are shifted and favored over the  $p$ -wave solution. This fact leads to an interesting feature, namely, at fixed band-filling and coupling constants, decreasing the temperature from  $T_c^{(1)}$  defined as the critical temperature for a paramagnet - superconductor type transition, an additional second phase transition of superconductor - superconductor type appears at a lower temperature  $T_c^{(2)} < T_c^{(1)}$ . This is a first-order transition between two superconducting phases of different symmetry close to the phase boundary lines. A similar double transition between  $s$  - and  $d_{x^2-y^2}$ -wave states has been deduced by Dahm *et al.* in case of superconducting states emerging from spin-fluctuation mechanism.

Away from half-filling (Fig. 1(d)), the increasing value of doping modifies the  $p$ -wave region of the phase diagram, however, the rate of paramagnetic phase emergence as the function of  $T$  is strongly doping dependent. Furthermore, at a fixed value of the doping, for strong repulsive on-site interactions and not excessively low  $U_1 < 0$  values, the  $d_{x^2-y^2}$ -symmetry phase represents not only a possible solution but it is the most stable superconducting phase among all the solutions of the gap equation. Qualitatively similar behaviour has been conjectured in various circumstances (Mierzejewski and Zielinski, 1995, Gufan, Vereshkov, Toledano, Mettout, Bouzerar and Lorman, 1995). Concerning the spin and charge density wave states not taken explicitly into account in Fig. 1, we expect their influence to be minor in the non-paramagnetic domain of the phase diagram. In this respect we would like to note that the nesting condition is hindered by doping in general, so its effect is reduced at low temperatures (Inaba, Matsukawa, Saitoh and Fukuyama, 1996) and following this line, doping usually enhances the emergence of superconductivity (Scalapino, 1995, Iglesias, Bernhard and Gusmao, 1995).

### C. Nearest-neighbour interactions with more than nearest neighbour hopping terms

From this paragraph on, besides  $NN$  terms,  $NNN$  contributions are also incorporated in the model Hamiltonian. As a first step, in order to obtain a clear image about modifications arising in the phase diagrams *purely* due to the presence of hopping terms exceeding  $NN$  distance in range, all the previously used interaction terms are kept unchanged but a more complex kinetic energy contribution is introduced in the present paragraph. This step also enables us to get an overall picture on how properties related to superconductivity are modified by DOS effects due to long-range hopping, without mixing these effects with the effects of  $NNN$  two-particle interaction terms. To accentuate the relevance to high- $T_c$  materials, we considered a dispersion relation obtained as a tight-binding fit to normal state *ARPES* data taken on *Bi2212* with nonzero hopping elements up to the fifth neighbours. The numerical values of the used  $t_l$  terms can be found in Ref. (Fehrenbacher and Norman, 1995). Here we note, that this new, extended dispersion breaks the  $\delta \rightarrow -\delta$  symmetry of the phase diagrams and in what follows, only hole-doped cases are discussed.

To show the source of modifications due to the extension in the hopping range, we compared in Fig. 2 the dispersion containing only  $NN$ , and the dispersion containing higher order contributions as well. The insets present energy dispersions along different directions of the first Brillouin zone. At first glance hopping terms exceeding  $NN$  distance in range seem to represent negligibly small corrections (for example in the present calculation  $|t_2|/|t_1| \sim 0.25$  and  $|t_3|/|t_1| \sim 0.08$ ). This is not true, however, in the process of calculating thermodynamic averages, since their effects during  $\mathbf{k}$ -integrations are extraordinarily enhanced by the supplementary extrema introduced to the dispersion. As it can be seen, the characteristic change occurs at small  $\mathbf{k}$ 's in the vicinity of the origin, with the flattening of the dispersion in this region. This leads to the fact (comparing Fig. 2(e) and (f) with Fig. 2(b) and (c)) that the region where  $\mathcal{N}^{-1} \sim \partial\epsilon(\vec{k})/\partial\vec{k} \simeq 0$  holds, is much larger for the  $t_l \neq 0$  ( $l \leq 5$ ) case than in the  $t_l \neq 0$  ( $l \leq 1$ ) case. Note, that all the integrands within the expressions that must be evaluated are proportional to  $\mathcal{N}$ . As a consequence, main DOS effect contributions like van Hove singularities (Blumberg *et al.*), saddle points (Abrikosov, 1995) and peaks (Cappelluti and Pietronero, 1996) are strongly wiped out by taking  $t_l = 0$  for  $l \geq 2$ , a choice that could lead to completely misleading conclusions in connection with the studied materials.

To illustrate the effect of dispersion modifications presented in Fig. 2. on different quantities of interest, the ratio  $R = 2\Delta_0/k_B T_c$ , ( $\Delta_0$  is the zero temperature gap amplitude) versus doping is plotted in Fig. 3. for a stable  $d_{x^2-y^2}$ -symmetry superconducting state of the phase diagram. In this plot open triangles are calculated with the dispersion used in Sec. III B, while open circles are obtained applying the extended dispersion used in the present Section. The effect of hopping terms exceeding  $NN$  distance in range can easily be seen. Besides the clear absolute value differences we note that the curve connecting the open triangles has a minimum at about  $\delta = 0.1$ , while the other line takes its

least value at half filling ( $\delta=0.0$ ). Here we also would like to underline that the  $R \approx 5.0$  value in the optimally doped regime ( $\delta \approx 0.12$ ) qualitatively agrees with predictions of other authors (Abrikosov, 1995, Dagotto, Nazarenko and Moreo, 1995). Furthermore, Fig. 3. nicely illustrates that higher amount of doping leads to a greater value of  $R$ , an enhancement that is clearly increased by the  $t_l \neq 0$  ( $l \geq 2$ ) terms.

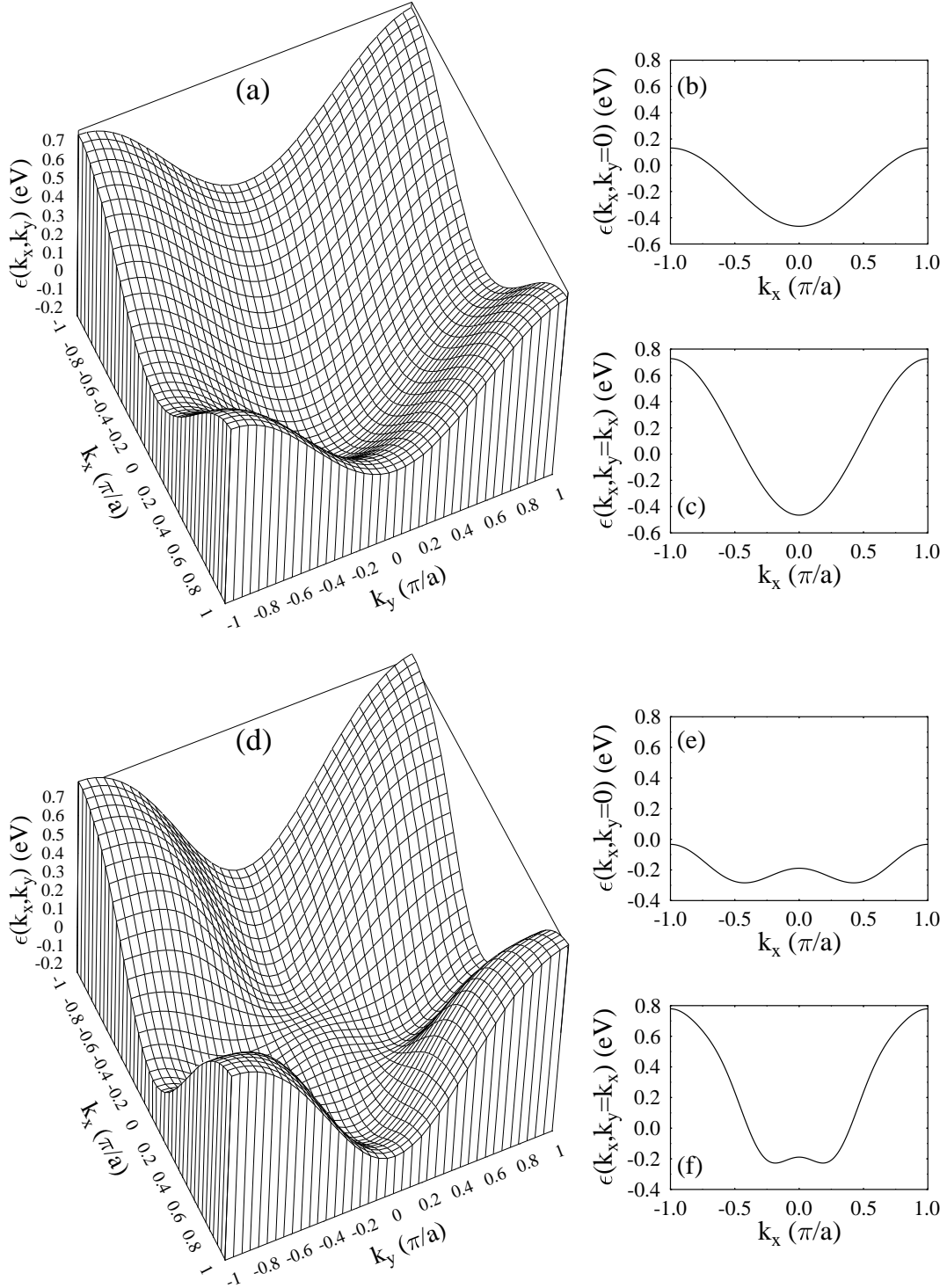


FIG. 2. Quasiparticle dispersion with nearest neighbour hopping terms [plot (a)] and beyond nearest neighbour hopping terms [plot (d)] in the first Brillouin zone. The insets show the dispersion in special directions, plots (b) and (e) are taken in the  $(\pi, 0)$  while plots (c) and (f) in the  $(\pi, \pi)$  directions.

Concerning the modifications produced in the phase diagram, the obtained results are exemplified at nonzero temperature ( $k_B T/W=0.005$ ) with Fig. 4(a) and (b) for  $\delta=0.0$  and  $\delta=0.2$ , respectively, which should be compared to Fig. 1(b) and (d) plotted at the same values of  $T$  and  $\delta$ . As it can be seen, the effects become more robust with increasing the doping. The extension of the  $A_1$ -symmetry domain becomes reduced and the  $d_{x^2-y^2}$  phase boundary is withdrawn more accentuatedly with increasing temperature in the presence of  $NNN$  hoppings.

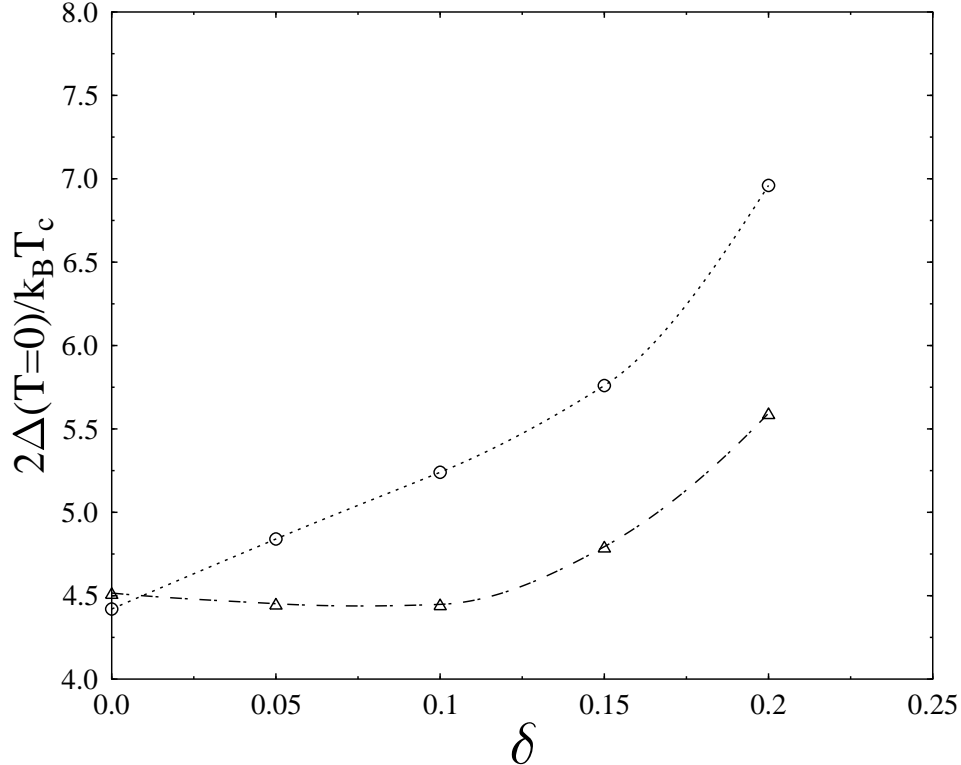


FIG. 3. Doping dependence of  $2\Delta(T=0)/k_B T_c$  for the stable  $d_{x^2-y^2}$  gap at a fixed set of coupling constants  $U_0=0.2W$ ,  $U_1=-0.15W$  and  $U_2=0.0$ . The calculated values are denoted by triangles and circles for the cases where only nearest neighbour and further than nearest neighbour hopping terms were taken into consideration, respectively.

All these theoretical results are perfectly compatible with and underline aspects observed in an increasing number of experimental data covering a large spectrum and suggesting the importance of  $NNN$  hopping contributions in building up superconducting properties: inelastic neutron scattering (Bourges, Regnault, Sidis and Vettier, 1996), magneto-resistance and conductivity (Mashimoto, Nakao, Kado and Koshizuka, 1996), thermopower, resistivity (Gasumyants, Ageev, Vladimirskaya, Smirnov, Kazanskiy and Kaydanov, 1996), and Hall effect (Hopfengartner, Leghissa, Kreiselmeier, Holzapfel, Schmitt and Ischenko, 1993) measurements. Theoretical support of this line (Capelluti *et al.*, Normand, H. Kohno and H. Fukuyama, 1996) is also present (see also the Introduction).

#### D. Influence of next-nearest neighbour interactions

From now on, the attention is focused on the changes in superconducting properties introduced by the nonzero value of  $NNN$  interactions. The dispersion used in Sec. III C has been kept unchanged for the present Section and  $NNN$  coupling with  $U_2 \neq 0$  has been considered. The obtained results regarding the superconducting phases at different temperature and doping values are shown in Fig. 5 and Fig. 6 for attractive and repulsive on-site interactions, respectively. Concerning the notations we would like to underline the following aspects. The presence of nonzero  $U_2$  term results in new singlet superconducting states characterized by  $\mathbf{k}$ -dependent order parameters proportional to  $\sin k_x \sin k_y$  or  $\cos k_x \cos k_y$  denoted by  $d_{xy}$  or  $s_{xy}$ , respectively, and new triplet superconducting states with  $(\sin k_x \cos k_y \pm \sin k_y \cos k_x)$  type of  $\mathbf{k}$ -dependence. For the last two states the  $p_2$ - and  $\bar{p}_2$ -wave notations are used. The symmetry classification of the new states can be found in Table I. In what follows, considering the phase



diagrams, the notation  $d_{xy}$  stands for an order parameter having  $B_2$  symmetry,  $d_{x^2-y^2}$  means an order parameter of  $B_1$  symmetry and the symbol  $A_1$  refers to an order parameter having  $s, s^*$  and  $s_{xy}$  components. Further notations are the same as in Fig. 1. In the presentation, for the sake of clarity, we concentrate on fixed values of  $U_0$  with opposite signs ( $U_0/W = -0.1$  and  $U_0/W = 0.1$  in Fig. 5 and Fig. 6, respectively), in order to maintain the two-dimensional structure of figures.

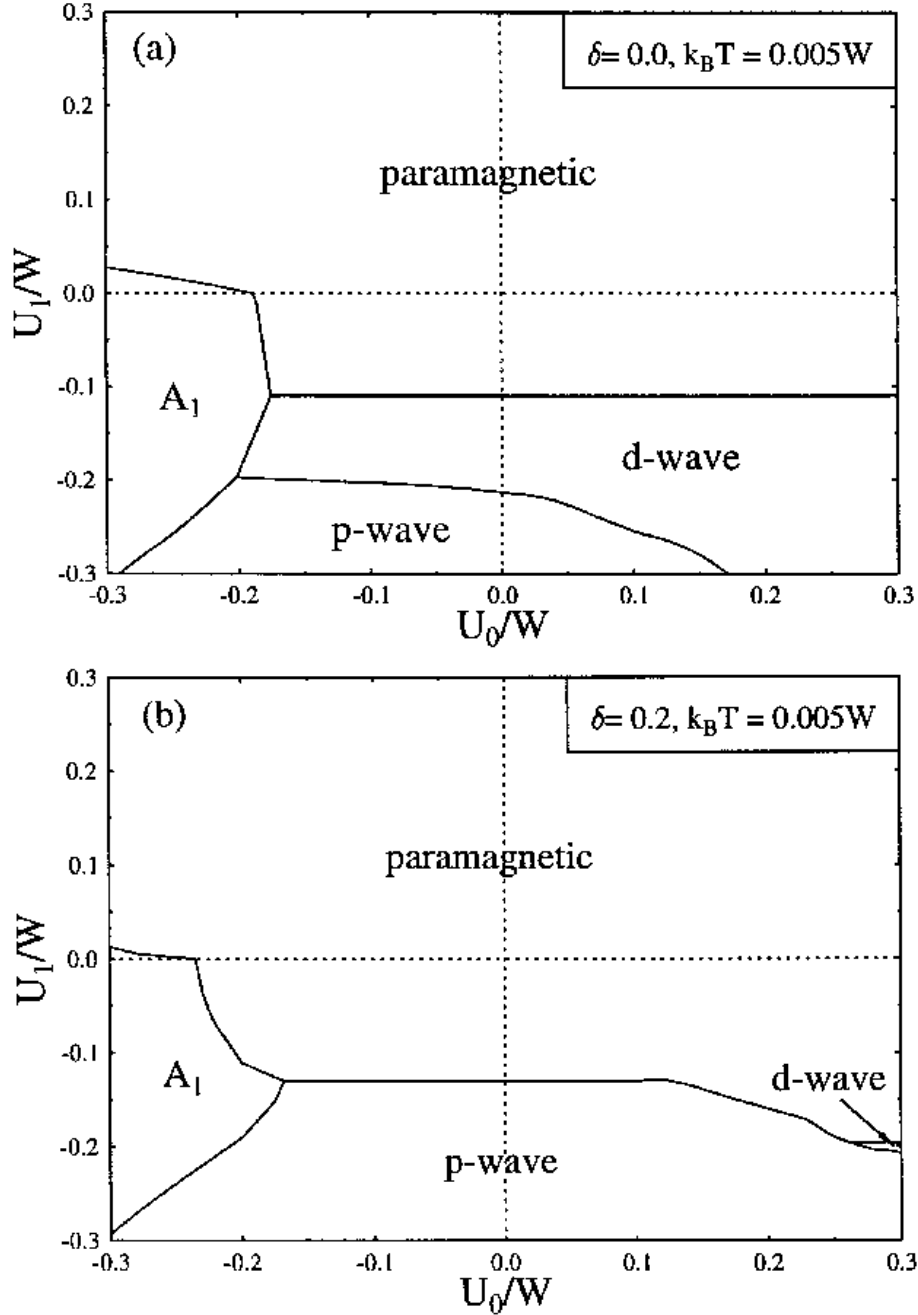


FIG. 4. Phase diagram at  $k_B T = 0.005W$  temperature for different dopings, using dispersion containing hopping terms beyond nearest neighbouring ones. Notations and curves have the same meaning as in Fig. 1.

The  $T = 0$  ground state phase diagram for different dopings ( $\delta = 0.0$  and  $\delta = 0.1$ ) in the presence of attractive on-site interaction presented in Fig. 5(a) and (c) shows a richness of different superconducting symmetry species. At this point we would like to emphasize the stability of the  $A_1$ -symmetry pairing state containing a coexistence of  $s^*$ ,  $s_{xy}$  and  $s$ -wave components. It is interesting to note that the  $s^*$  and  $s_{xy}$  components are governed by  $NN$  and  $NNN$

interaction, respectively, while the conventional  $s$ -wave part is primarily determined by the on-site interaction. As a consequence, despite the repulsive intersite couplings, the  $A_1$ -symmetry superconducting phase stabilizes due to the compensation of repulsions by the on-site attraction. In this compensation doping is of great importance, since a small increase in its value induces the emergence of  $A_1$ -symmetry pairing state in the non-superconducting region of the phase diagram, as shown in Fig. 5(c).

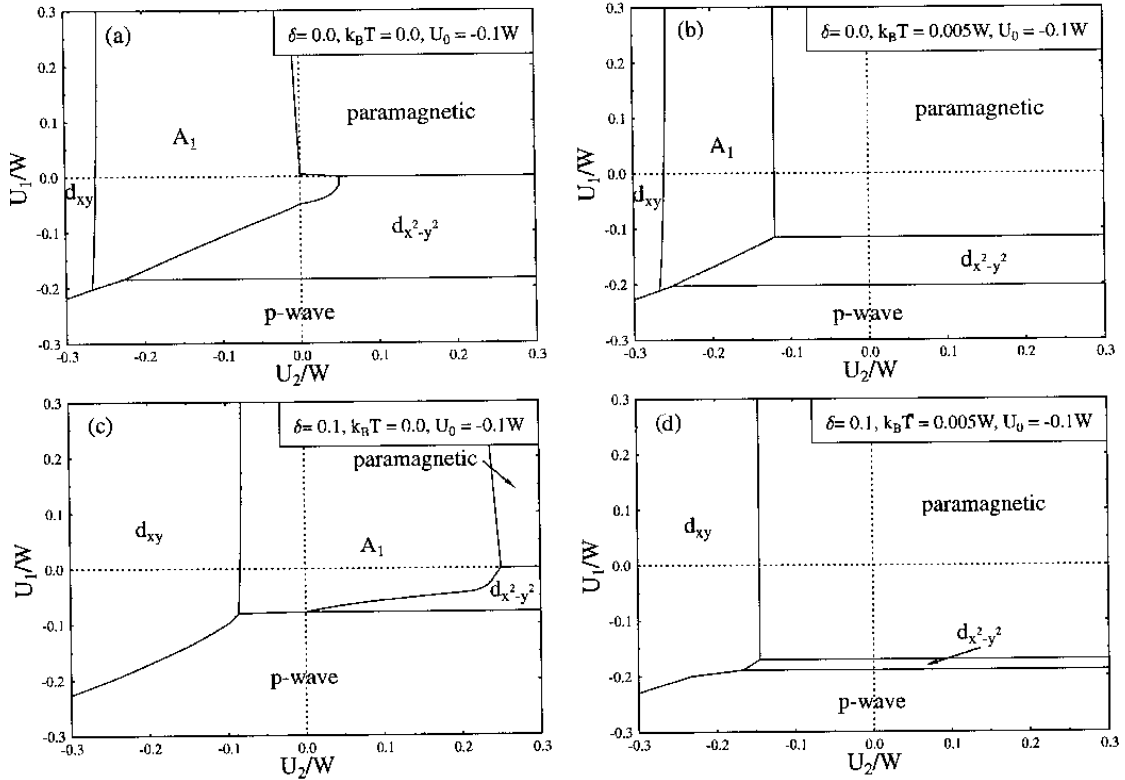


FIG. 5. Phase diagram with next-nearest neighbour couplings at zero ( $k_B T = 0.0$ ) and nonzero ( $k_B T = 0.005W$ ) temperatures for different dopings and fixed on-site attraction,  $U_0 = -0.1W$ , for a dispersion containing also hopping terms beyond nearest neighbouring ones. Dotted lines mean coordinate axis and solid lines represent boundaries between different symmetry phases. The meaning of notations  $d_{x^2-y^2}$ ,  $d_{xy}$ ,  $A_1$ ,  $p$ -wave and *paramagnetic* is the same as in the text.

The structure of the phase diagram at a higher, nonzero temperature is exemplified in Fig. 5(b) and (d). While the  $A_1$  phase is rapidly destroyed by increasing the temperature, the  $d_{xy}$  phase entirely induced by  $NNN$  terms shows a more accentuated resistance against thermal pair-breaking effects. In this way, for large values of  $|U_2|/W$  the stability of the  $d_{xy}$ -symmetry pairing state can be coherently deduced within the presented model, a fact that underlines the correctness of the conjecture made by Fehrenbacher and Norman (Fehrenbacher *et al.* related to the stability of the  $d_{xy}$  state).

Concerning triplet pairing we note that the states with  $\tilde{p}$ -,  $p_2$ - and  $\tilde{p}_2$ -symmetry never have lower free-energy in the coupling constants' space under study than the triplet pairing state of standard  $p$ -wave symmetry.

If now the  $U_0 > 0.0$  case is considered, the phase diagram significantly changes, as it is shown in Fig. 6. The most important feature of this figure is, that the  $A_1$ -symmetry solution never reaches the level of a stable superconducting state within the analyzed  $U_2$  region for  $|U_1| \ll 1.0$  for slight dopings. This result is in accordance with the observation of Fehrenbacher *et al.*, where it is claimed that in the presence of on-site repulsion with small  $NNN$  attractions ( $|U_2|/W \ll 1.0$ ), the stable superconducting state of  $A_1$ -symmetry can be realized in the limit of  $|U_1| \rightarrow 0.0$  only at relatively high values of the doping.

Figure 6(a) and (c) show the  $T=0$  phase diagram of the model with  $U_0=0.1W$  at two doping values ( $\delta=0.0$  and  $\delta=0.1$ ) in the  $(U_1/W, U_2/W)$  plane. The phase boundary between the  $d_{x^2-y^2}$  and  $d_{xy}$  phases moves slowly into the domain of  $d_{x^2-y^2}$  phase with increasing values of the doping, that is, higher doping favors states of  $d_{xy}$ -symmetry over states of  $d_{x^2-y^2}$ -symmetry. Furthermore, as it can be observed in Fig. 6(a) and (c), the  $d_{x^2-y^2}$ - $d_{xy}$  phase boundary is linear and strongly affected by doping. For small values of  $\delta$  it coincides with the  $U_1 = \alpha U_2$  line with  $\alpha \simeq 1.0$ , while

for larger doping values it is shifted away and  $\alpha$  becomes smaller than 1.0. This leads to the following interesting feature: changing the doping continuously the symmetry of the stable superconducting state changes and a transition between the two different  $d$ -like pairing states (from  $B_2$ -symmetry to  $B_1$ -symmetry) takes place for small, fixed values of the coupling constants. This transition line within the  $T=0$  phase diagram, suggested by detailed investigations, is of first order.

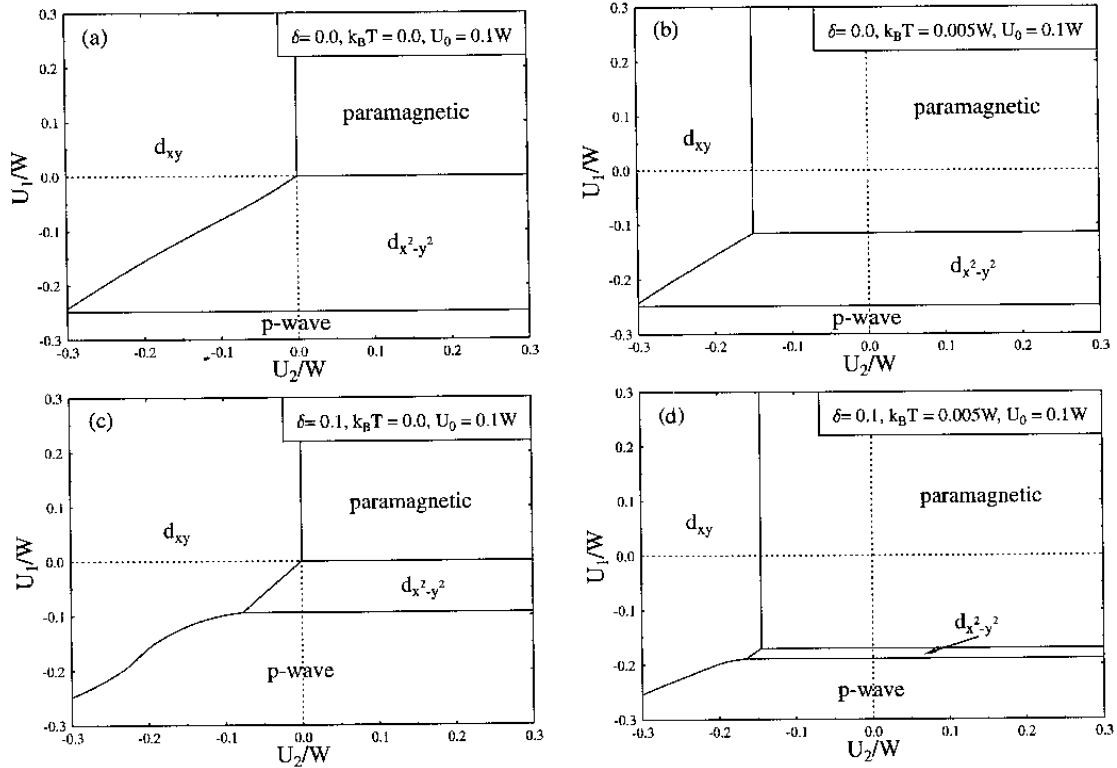


FIG. 6. Phase diagram with next-nearest neighbour couplings at zero ( $k_B T = 0.0$ ) and nonzero ( $k_B T = 0.005W$ ) temperatures for different dopings and fixed on-site repulsion,  $U_0 = 0.1W$ , for a dispersion containing also hopping terms beyond nearest neighbouring ones. Notations and curves have the same meaning as in Fig. 5.

Examining phase boundaries between the  $p$  and  $d_{xy}$  or  $d_{x^2-y^2}$  superconducting states, one can see them moving upward with increasing doping into the  $d_{x^2-y^2}$ -symmetry phase. However, large  $NNN$  interaction ( $|U_2|/W \gg 1$ ) and small  $NN$  attraction ( $|U_1|/W \ll 1$ ) favors superconducting pairing state of  $d_{x^2-y^2}$  or  $d_{xy}$  symmetry, depending on the sign of  $U_2$ , an observation that holds even for heavily doped systems.

Turning now to the  $T \neq 0$  case depicted in Fig. 6(b) and (d), it can be observed that the triple-point moves downward in the  $U_1, U_2 < 0.0$  region with increasing the temperature. The phase boundary of the  $d_{x^2-y^2}$  phase modifies more rapidly with increasing  $T$ , suggesting that in the large  $|U_2|$  region (with  $U_2/W < 0.0$  and  $|U_1|/W \ll 1.0$ ) the highest critical temperature can be reached with a  $d_{xy}$  phase. The stability of the  $d_{xy}$  phase against thermal fluctuations, in comparison with the same stability of  $d_{x^2-y^2}$  phase, is again striking.

In the light of Figs. 5 and 6, one can conclude that small  $|U_1|/W$  and large attractive  $NNN$  coupling  $U_2$  favors  $d_{xy}$  pairing, while small  $|U_2|/W$  and strong attractive  $NN$  coupling  $U_1$  gives rise to stable  $d_{x^2-y^2}$  pairing. These results emphasize the correctness of the conjecture made by Wenger and Östlund (Wenger *et al.*) related to the stability of different  $d$  symmetry species, who also claimed that third-neighbour attractive interaction could lead to a stable  $\mathbf{k}$ -dependent  $s$ -wave within the phase diagram, especially in the presence of repulsive closer-neighbour interactions.

The electron doping versus hole doping behaviour is exemplified with Fig. 7, where doping dependence of gap amplitudes and free-energy are shown for a certain set of coupling constants. Having a glance at Fig. 7(a) one can see that besides the gap amplitudes, phase also changes (i.e. sign change of  $\Delta_i$  in the presented figure) emerge for different solutions at a critical value of doping. More interestingly, Fig. 7(b) predicts the stable superconducting state to have  $A_1$ -symmetry in the electron doped regime even for repulsive on-site couplings. This suggests that the symmetry of the pairing state in electron doped materials (for example in *NCCO*) might be explained without assuming attraction

in the on-site interaction channel. Systematic study of the electron doped case is under progress.

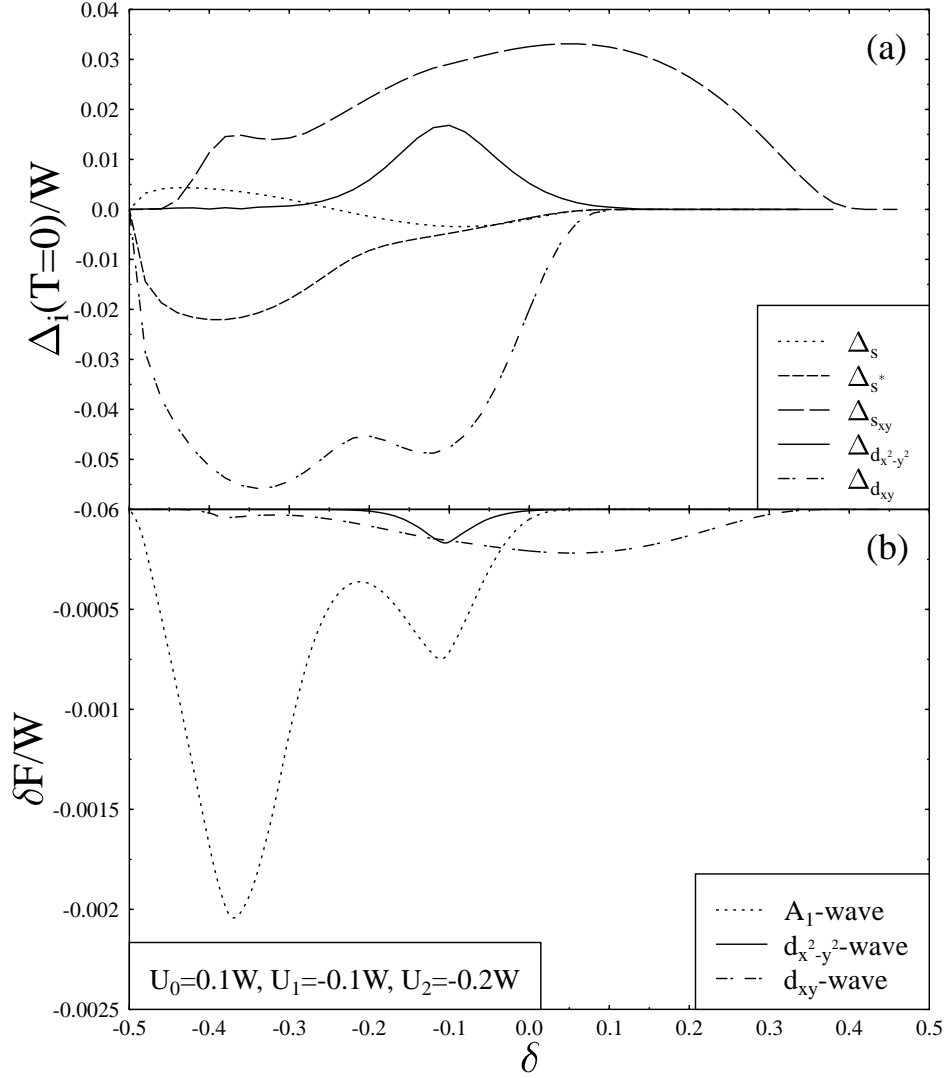


FIG. 7. Doping dependence of gap amplitudes [plot (a)] and of corresponding free-energies [plot (b)] at a fixed set of coupling constants  $U_0=0.1W$ ,  $U_1=-0.1W$ ,  $U_2=-0.2W$  for the dispersion containing hopping terms beyond nearest neighbouring ones.

In Fig. 8 we focus our attention on the effects accentuated by  $NNN$  interaction terms in  $T_c$ , in zero temperature gap-amplitude and in the ratio of  $R = 2\Delta_0/k_B T_c$ . For simplicity,  $U_1$  is set to be zero in this study. This particular choice results in an order parameter of the form  $\Delta(\vec{k}) = \Delta_s + \Delta_{s_{xy}} \cos k_x \cos k_y$ , (i.e. only  $s$  and  $s_{xy}$  components). The values of  $U_0$  and  $U_2$  are tuned so that the emerging  $A_1$ -symmetry pairing state becomes the stable superconducting state for the chosen set of interaction parameters. The effect of  $U_2$  on the mentioned quantities is presented in the figure. We note, that for  $U_1 \neq 0.0$  values a similar analysis can be done leading essentially to the same features.

First of all, Fig. 8(a) shows the  $U_2$  dependence of the gap amplitudes at zero temperatures. One can immediately realize the exponential type behaviour of  $\Delta_{s_{xy}}$  versus  $-U_2$  for small,  $|U_2|/W \ll 1.0$  values. At the same time,  $\Delta_s$  has a linear dependence on  $-U_2$ . The  $U_2$  dependence of the critical temperature is exemplified in Fig. 8(b) for the  $A_1$ -symmetry solution. A good fit to the numerically calculated points can be obtained by the  $T_c \sim \exp[-1/(K\sqrt{U_2})]$  relation, where  $K=0.5226$ . Such type of  $T_c$  behaviour related to non-on-site interactions is not unusual. For example, a similar relation was suggested by Dahm *et al.* (Dahm *et al.*) for the nearest neighbour coupling dependence of  $T_c$ , instead of an  $\exp[-1/(\tilde{K}g_i)]$  functional form. Concerning the ratio of the zero temperature gap amplitude to  $T_c$ , in Fig. 8(c) the  $R=2\Delta_0/k_B T_c$  values are plotted versus  $-U_2/W$  for the two components of the  $A_1$  solution. In the  $U_2=0$

case (where the order parameter has the form of  $\Delta(\vec{k}) = \Delta_s$ ) this ratio is about 3.52 and hence corresponds to the *BCS* predicted value. However, if *NNN* interaction is turned on an  $s_{xy}$  component of the order parameter develops rapidly resulting in an increase (decrease) of the ratio  $R$  for the  $s_{xy}$  ( $s$ ) channel.

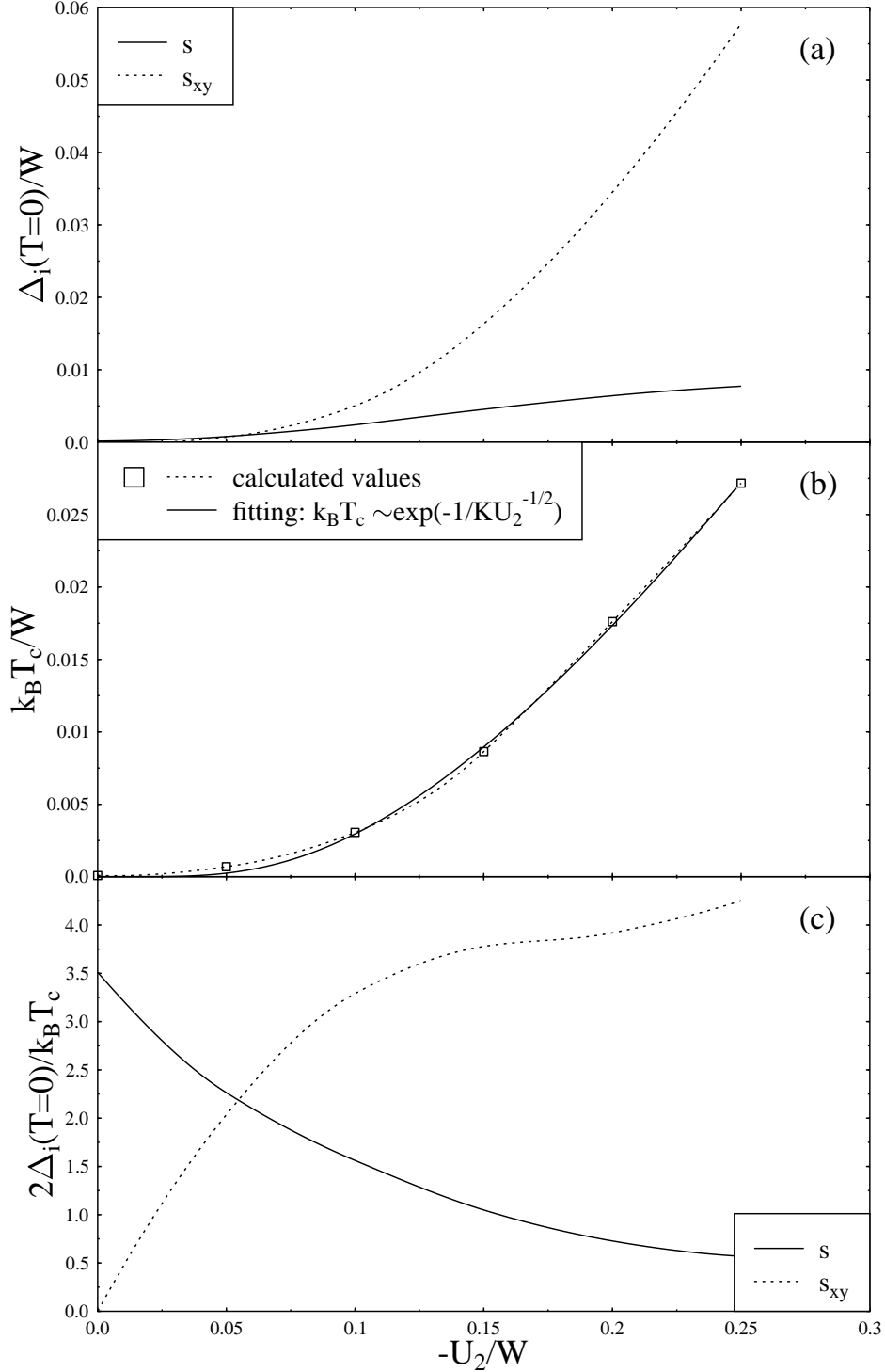


FIG. 8. The effect of  $U_2$  on components of a stable  $A_1$ -symmetry solution at  $U_0 = -0.1W$ ,  $U_1 = 0.0$  at half-filled band; plot (a) shows the zero temperature gap amplitude versus  $U_2$  dependence, plot (b) depicts  $U_2$  dependence of the critical temperature while plot (c) illustrates  $U_2$  dependence of the ratio  $2\Delta(T=0)/k_B T_c$ .

Based on these results it can be seen that nonzero next-nearest neighbour coupling, besides the emergence of different possible superconducting species, also influences the main characteristic properties of the superconducting phase.

#### IV. SUMMARY AND CONCLUSIONS

The superconducting phase diagram of the two-dimensional extended Hubbard model containing hopping and interaction terms with spatial dependences exceeding nearest neighbour distance in range has been systematically analyzed in mean-field approximation. The possible superconducting phases of different symmetry were taken into account unrestrictedly. For building up the phase diagrams, the emerging phase was chosen on the basis of a free-energy (or at  $T = 0$  ground state energy) analysis of all the possible solutions of the gap equations for every fixed set of coupling constants, temperature and doping values. Main characteristics of different superconducting phases including critical temperatures  $T_c$ , zero temperature gap amplitudes  $\Delta_0$ ,  $\Delta_0/T_c$  ratios, temperature and doping dependences were also studied in detail for every domain of the phase diagram. The obtained results clearly underline the importance of next nearest neighbour terms (both hopping and interaction contributions) in determining the prominent superconducting properties of the system.

The present paper explored such a parameter domain of the phase diagram which has not been investigated so far systematically in literature starting with Fig. 1, where in the presence of only nearest neighbour terms, non half-filled band case was also investigated. Starting from this level different next-nearest neighbour contributions were taken gradually into consideration within the extended Hubbard Hamiltonian, their effects being systematically presented in Figs. 2-8 and analyzed in detail with physical implications being emphasized, especially those connected to the presence of next-nearest neighbour terms.

On this line the following interesting features deserve attention: double phase transitions with decreasing temperature (following the emergence of a superconducting state at  $T_c^{(1)}$  the symmetry of the superconducting order parameter changes at  $T_c^{(2)} < T_c^{(1)}$  in a first-order phase transition); quantum phase transitions at zero temperature between pairing states of different symmetry driven by doping; enhancement in the resistance of the stable superconducting phase against thermal pair-breaking effects in the presence of interaction terms exceeding nearest neighbour distance in range; increase in the  $T = 0$  gap-amplitude over  $T_c$  ratio for some symmetry species; the main superconducting properties become more sensible with respect to doping; strong asymmetry between hole and electron doped cases; rich spectrum of stable superconducting states of different symmetry (in the presence of repulsive on-site and in some cases even for repulsive nearest neighbour interactions, the  $A_1$  symmetry is favored for electron, and a  $d$ -wave type order parameter for hole doping values); elimination of  $\mathbf{k}$ -independent order parameters even at half-filling, and so on.

We strongly hope, that the presented results will constitute a valuable starting point for further theoretical investigations related to the effect of long-range contributions in building up superconducting properties of the system under study.

#### V. ACKNOWLEDGEMENTS

One of the authors (Zs.Sz.) would like to acknowledge earlier financial support by SOROS Foundation and present financial supports of the Universitas and the Pro Regione Foundations of Kossuth Lajos University. For Zs.G. research was supported by the Hungarian National Science Funds under grant OTKA-T013952. Furthermore, both authors thank financial support of the Research Group in Physics of the Hungarian Academy of Sciences at Kossuth Lajos University, Debrecen.

#### VI. REFERENCES

- P. W. Anderson, Science **235** (1987) 1196.
- E. Dagotto, Rev. Mod. Phys. **66** (1994) 763.
- M. G. Smith, A. Manthiram, J. Zhou, J. B. Goodenough and J. J. Market, Nature **351** (1991) 549.
- R. Micnas, J. Ranninger, and S. Robaszkiewicz, Rev. Mod. Phys. **62** (1990) 113.
- See for example Proc. Inter. Conf. on Strongly Correlated Electron Systems, Amsterdam 1994, SCES-94, edited by F. R. de Boer, P. F. de Chatel, J. J. M. Franse and A. de Visser, North-Holland, Elsevier, 1995.
- J. de Boer, V. E. Korepin and A. Schadschneider, Phys. Rev. Lett. **74** (1995) 789.

T. Koma and H. Tasaki, Phys. Rev. Lett. **68** (1992) 3248.  
H. Tasaki, Phys. Rev. Lett. **75** (1995) 4678.  
J. A. Verges, F. Guinea, J. Galan, P. G. J. van Dongen, G. Chiappe and E. Louis, Phys. Rev. **B49** (1994) 15400.  
A. F. Veilleux, A. M. Daré, L. Chen, Y. M. Vilk and A. M. S. Tremblay, Phys. Rev. **B52** (1995) 16255.  
M. Lavagna and G. Stemmman, Phys. Rev. **B49** (1994) 4235.  
P. B. Littlewood, J. Zaanen, G. Aeppli and H. Monien, Phys. Rev. **B48** (1993) 487.  
G. Blumberg, B. S. Stojkovic and M. V. Klein, Phys. Rev. **B52** (1995) R15741.  
M. Gulácsi, A. R. Bishop and Zs. Gulácsi, Physica **C244** (1995) 87.  
A. A. Abrikosov, Phys. Rev. **B51** (1995) 11955 and ibid., **B52** (1995) R15738, Physica **C222** (1994) 191 and ibid., **C233** (1994) 102.  
V. Ponnambalam and U. V. Varadaraju, Phys. Rev. **B52** (1995) 16213.  
R. Fehrenbacher and M. R. Norman, Phys. Rev. Lett. **74** (1995) 3884.  
C. O'Donovan and J. P. Carbotte, Phys. Rev. **B52** (1995) 16208.  
W. Brenig, Physics Reports **251** (1995) 155.  
R. Strack and D. Vollhardt, Phys. Rev. Lett. **72** (1994) 3425.  
R. Strack and D. Vollhardt, Jour. Low Temp. Phys. **99** (1995) 385.  
C. Verdozzi and M. Cini, Phys. Rev. **B51** (1995) 7412.  
C. Verdozzi, in NATO Advanced Study Institute Series B, Physics, 1993, Kluwer and Dordrecht, page 237.  
D. M. King et al. Phys. Rev. Lett. **70** (1993) 3159  
M. Di Stasio and X. Zotos, Phys. Rev. Lett. **74** 2050, (1995).  
J. van den Brink, M. B. J. Meinders, J. Lorenzana, R. Eder and G. A. Sawatzky, Phys. Rev. Lett. **75** (1995) 4658.  
G. Grigelionis, E. E. Tornau and A. Rosengren, Phys. Rev. **B53** (1996) 425.  
A. P. Kampf, Physics Reports, **249** (1994) 222.  
A. A. Abrikosov, L. P. Gor'kov and I. E. Dzyaloshinskii, in Methods of Quantum Field Theory in Statistical Physics (*Pergamon Press Ltd.*, 1965).  
T. Dahm, J. Erdmenger, K. Schanberg and C. T. Rieck, Phys. Rev. **B48** (1993) 3896.  
B. L. Gyorffy, J. B. Staunton and G. M. Stocks, Phys. Rev. **B44** (1991) 5190.  
W.H Press, S.A. Teukolsky, W.T. Vetterling and B.P. Flannery: Numerical Recipes in Fortran (*Cambridge University Press*, 2nd edition, 1992).  
R. Micnas, J. Ranninger, S. Robaszkiewicz and S. Tabor, Phys. Rev. **B37** (1988) 9410.  
R. Micnas, J. Ranninger and S. Robaszkiewicz, Phys. Rev. **B39** (1989) 11653.  
F. Wenger and S. Östlund, Phys. Rev. **B47** (1993) 5977.  
S. Zhang, Phys. Rev. **B42** (1990) 1012.  
M. Mierzejewski and J. Zielinski, Phys. Rev. **B52** (1995) 3079.  
Y. M. Gufan, G. M. Vereshkov, P. Toledano, B. Mettout, R. Bouzerar and V. Lorman, Phys. Rev. **B51** (1995) 9228.  
M. Inaba, H. Matsukawa, M. Saitoh and H. Fukuyama, Physica **C257** (1996) 299.  
D. J. Scalapino, Physics Reports **250** (1995) 331.  
J. R. Iglesias, B. H. Bernhard and M. A. Gusmao, Physica **B206-207** (1995) 678.  
E. Cappelluti and L. Pietronero, Phys. Rev. **B53** (1996) 932.  
E. Dagotto, A. Nazarenko and A. Moreo, Phys. Rev. Lett. **74** (1995) 310.  
P. Bourges, L. P. Regnault, Y. Sidis and C. Vettier, Phys. Rev. **B53**, (1996) 876.  
K. Mashimoto, K. Nakao, H. Kado and N. Koshizuka, Phys. Rev. **B53** (1996) 892.  
V. E. Gasumyants, N. V. Ageev, E. V. Vladimirskaia, V. I. Smirnov, A. V. Kazanskiy and V. I. Kaydanov, Phys. Rev. **B53** (1996) 905.  
R. Hopfgartner, M. Leghissa, G. Kreiselmeyer, B. Holzapfel, P. Schmitt and G. S. Ischenko, Phys. Rev. **B47** (1993) 5992.  
B. Normand, H. Kohno and H. Fukuyama, Phys. Rev. **B53** (1996) 856.